Editors' Suggestion | Featured in Physics

Two-Particle Interference with Double Twin-Atom Beams

F. Borselli,[1] M. Maiwöger,[1] T. Zhang,[1] P. Haslinger,[1] V. Mukherjee,[2] A. Negretti,[3] S. Montangero,[4,5] T. Calarco,[6] I. Mazets,[1,7] M. Bonneau,[1] and J. Schmiedmayer[1]

[1]*Vienna Center for Quantum Science and Technology, Atominstitut, TU Wien, 1020 Vienna, Austria*
[2]*Indian Institute of Science Education and Research, 760010 Berhampur, India*
[3]*The Hamburg Centre for Ultrafast Imaging, Universität Hamburg, D-22761 Hamburg, Germany*
[4]*Dipartimento di Fisica e Astronomia "G. Galilei," Università di Padova, I-35131 Padova, Italy*
[5]*INFN Sezione di Padova, I-35131 Padua, Italy*
[6]*Forschungszentrum Jülich, Wilhelm-Johnen-Straße, D-52425 Jülich, Germany and University of Cologne, Institute for Theoretical Physics, D-50937 Cologne, Germany*
[7]*Research Platform MMM "Mathematics–Magnetism–Materials," c/o Fakultät für Mathematik, Universität Wien, 1090 Vienna, Austria*

(Received 3 October 2020; revised 9 December 2020; accepted 13 January 2021; published 23 February 2021; corrected 10 May 2021)

We demonstrate a source for correlated pairs of atoms characterized by two opposite momenta and two spatial modes forming a Bell state only involving external degrees of freedom. We characterize the state of the emitted atom beams by observing strong number squeezing up to −10 dB in the correlated two-particle modes of emission. We furthermore demonstrate genuine two-particle interference in the normalized second-order correlation function $g^{(2)}$ relative to the emitted atoms.

DOI: 10.1103/PhysRevLett.126.083603

Correlated and entangled pairs constitute a fundamental tool in the hands of a quantum engineer [1] with a wide range of possible applications, from probing fundamental questions regarding the nature of the quantum world, to building blocks for quantum communication and quantum computers, to sensors and development of metrological devices [2]. Many beautiful fundamental and applied experiments have been performed with entangled pairs of photons [3]. In recent years huge progress was made in creating entangled states of massive particles, most prominently in the context of developing fundamental building blocks for quantum logic operations. The interest is also motivated by performing a Bell test using massive particles, as in spin correlations between protons [4], electrons [5], ions [6], Josephson phase qubits [7], and atoms [8].

The above experiments were performed for internal states, furthermore all except the proton experiment employed localized systems. Here we will focus on external degrees of freedom of freely propagating pairs of atoms. The most direct way to produce them is by collisions, which can either be accomplished by collisional deexcitation in a quantum degenerate sample in an excited motional state in a trap or waveguide [9], by designing the dispersion relation using a lattice [10–12], or by colliding two condensates with different momenta and looking at the scattering halo [13,14].

In this Letter, we present a source of double twin-atom beams (DTBs): beams of atoms emitted in pairs with opposite momenta (twin atoms) traveling in a double waveguide potential. This has two advantages. On the one hand, it forces the emission along the waveguide; hence it is more efficient than experiments where the emission happens in free space [13,15,16]. On the other hand, the presence of two such parallel waveguides allows the possibility for the twin pair to be emitted into either the left waveguide (L waveguide) or into the right waveguide (R waveguide); hence an entangled state of two atoms only involving motional degrees of freedom is possible. We measure momentum correlations between the atoms in the pairs and observe a fringe pattern in the normalized second-order correlation function $g^{(2)}$ that stems from a two-particle interference phenomenon. The fundamental idea at the basis of this experiment is discussed in more detail in Ref. [17].

Our experiment starts with preparing a one-dimensional (1D) quasi-Bose-Einstein Condensate (BEC) [18] of 600–2000 atoms ($T \lesssim 40$ nK) magnetically trapped in a tight transverse anharmonic potential ($\nu_{y,z} \simeq 2$ kHz) with a shallow longitudinal harmonic confinement ($\nu_x \simeq 10$ Hz) created below an atom chip [19]. The experimental procedure to create the DTBs [Figs. 1(a) and 1(b)] begins with splitting the 1D trapping potential into a double-well potential [20]. The splitting ramp is designed by optimal control to achieve *state inversion*, that is, the 1D quasi-BEC is transferred to the second transversely excited state of the double-well potential, the desired *source state*. In particular, a potential barrier with a time-varying height is first created along the y axis. During a certain time interval, the barrier height is lifted up and down symmetrically with respect to the minima of the two wells and finally settled at a value which determines the final double-well geometry.

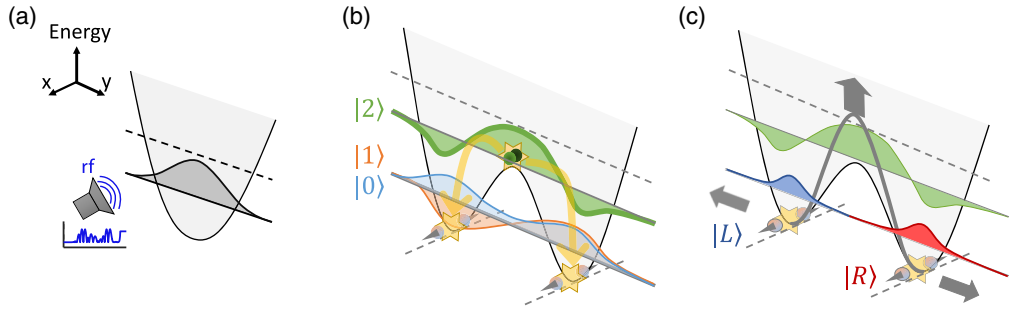

FIG. 1. Sketch of the experimental procedure. (a) The quasi-BEC (gray) lies initially in the transverse ground state of a single-well potential characterized by a tightly confined direction (y axis or transverse axis) and a weakly confined direction (x axis or longitudinal axis, potential curve along this axis not displayed). An rf field with variable amplitude is used to excite the condensate and at the same time reach a double-well configuration along the y axis. (b) The final double-well potential with its vibrational states along the y axis: the second-excited state (green), which constitutes the *source state*, the first-excited (orange), and the ground state (blue) are defined by $|n_y\rangle$, where $n_y = 0, 1, 2$ is the vibrational quantum number. Two atoms from the source state can collide and decay into a twin pair (opposite momenta along the x axis). Since the atoms in the twin pair can be emitted either in the symmetric $|0\rangle$ (blue) or the antisymmetric $|1\rangle$ (orange) transverse state, we define the emitted two-particle state as double twin-atom beam (DTB) state. (c) The DTB state can also be expressed in terms of the localized left- $|L\rangle$ (blue curve) and right-well state $|R\rangle$ (red curve). The gray arrows represent the process of quickly lifting up the barrier height and pushing the well's minima away from each other.

When the amplitude of the rf field is increased, the distance between the two minima increases. The manipulation of the transverse potential is achieved by radio-frequency dressing [21,22]. The precise amplitude of the applied rf field is determined by optimal-control techniques (see Supplemental Material [23]).

The final potential along the y axis is displayed in Fig. 1(b), together with the corresponding single-particle eigenstates. The states are labeled $|n_y\rangle$ with the vibrational quantum number along the y axis $n_y = 0, 1, 2$ (since along the other transverse direction $n_z = 0$ during the whole experiment, we have dropped the corresponding index). The second excited state (green) $|2\rangle$ has an energy $\epsilon/h = \nu_2 - \nu_0 \simeq 1.3$ kHz and represents the source state. The two lowest eigenstates, $|0\rangle$ (light blue) and $|1\rangle$ (orange), have an energy difference $E_1 - E_0 \ll \min\{\epsilon, \mu\}$, where μ is the chemical potential [31], and thus are assumed to be degenerate. In Fig. 1(c), the localized left- $|L\rangle$ and right-well state $|R\rangle$ of the double-well potential are displayed (blue and red curves ,respectively). The two basis representations are linked by the relations $|0\rangle = (|L\rangle + |R\rangle)/\sqrt{2}$ and $|1\rangle = (|L\rangle - |R\rangle)/\sqrt{2}$.

A binary collision between two atoms in the source state can lead to the emission of a pair of twin atoms (for an extensive study of the emission process, see Ref. [32]). Because of momentum conservation, the atoms are emitted with opposite momenta along the shallow longitudinal direction (x axis), which constitutes the first pair of modes available to each indistinguishable atom. The residual potential energy ϵ from the source state gets translated into kinetic energy of the emitted twin pairs. This determines a selection of only two longitudinal momenta $\pm k_0 = \pm\sqrt{2m\epsilon}/\hbar$. Furthermore, the presence of a double-well potential along the tightly confined transverse direction (y axis) defines an additional spatial degree of freedom represented by the left $|L\rangle$ and right state $|R\rangle$ in Fig. 1(c), thus bringing to four the total number of modes available to each indistinguishable atom.

The twin pair is created by s-wave scattering (δ-function interaction) between two bosonic atoms in the source state and emitted along the symmetric double waveguide with negligible overlap between the $|L\rangle$ and $|R\rangle$ states. For bosonic particles the state of the atom pair is expected to be in the maximally entangled state:

$$|\Psi_{\mathrm{DTB}}\rangle = \frac{1}{\sqrt{2}}(|L\rangle_-|L\rangle_+ + |R\rangle_-|R\rangle_+), \tag{1}$$

where $|i\rangle_-|i\rangle_+ \equiv |i\rangle_{-k_0} \otimes |i\rangle_{+k_0}$ and $i = \{L, R\}$ (for details on the calculation leading to this result, see the Supplemental Material [23]). Such a two-particle state is hereafter denoted as DTB state.

Experimental evidence will be provided hereafter in favor of the generation of the state in Eq. (1). First, in the so-called *separation procedure* we will measure the classical correlations among the different four single-particle modes. To do so, we quickly increase the potential barrier separating the two waveguides before the trap is switched off. This imparts a large and opposite transverse momentum onto the L- and R-well states, so that they can be counted separately. The correlation analysis then lets us to exclude the emission of $|L\rangle_-|R\rangle_+$ and $|R\rangle_-|L\rangle_+$ pairs. However, the same analysis cannot exclude the presence of mixed states of $|L\rangle_-|L\rangle_+$ and $|R\rangle_-|R\rangle_+$ with no coherent superposition. Therefore, in the so-called *interference procedure* we release the atomic wave functions of the emitted beams from the two waveguides; they transversally expand, overlap, and interfere. A second-order correlation analysis will then reveal coherent superposition between a

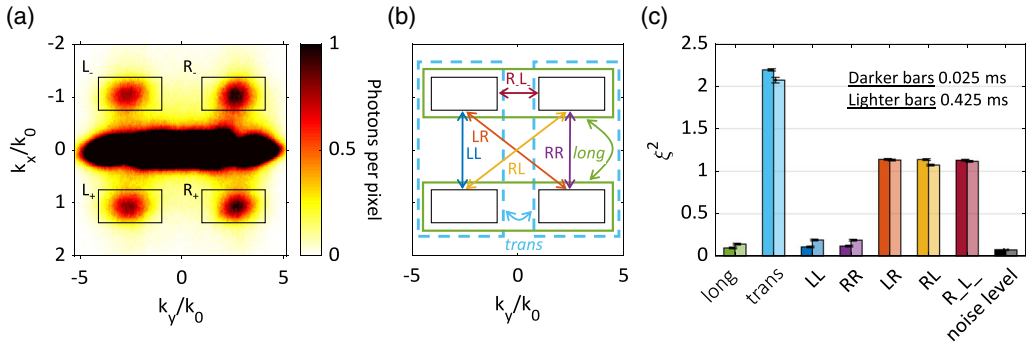

FIG. 2. Intramode correlations. (a) Experimental fluorescence image averaged over 825 experimental runs obtained with the separation procedure. Each run involves 2000–2200 total atoms, in average 150 of which are DTB atoms (75 pairs). The long time of flight makes the initial y-axis momentum distribution accessible (see Supplemental Material [23]). The central cloud corresponds to the source state, while the emitted DTB atoms are found at $\pm k_0$. The black boxes define the regions used for the correlation analysis. (b) Color scheme definition of the different combinations of DTB modes considered. (c) Histogram of different number-squeezing values ξ^2 for each combination of DTB modes defined in (b).

pair being emitted into the L waveguide and the same pair being emitted into the R waveguide, hence excluding the presence of only mixed states of such twin pairs. Moreover, the specific quantum superposition detected in this experiment is consistent with the predicted zero relative phase between the L and R twin pairs in Eq. (1).

Independently of the experimental procedure, the trap is held for a certain holding time t_{hold}. The BEC undergoes a free-fall stage and expands for a time of flight of 44 ms before the atoms are detected by traversing the light sheet of our single atom imaging detector [33]. Because of the long time of flight, the image shows the y axis *in situ* momentum distribution of the atoms (see Supplemental Material [23]).

Separation procedure.—In order to resolve the transverse states, we imprint an extra transverse acceleration. This is done by a quick rise of the potential barrier between the L and R well [Fig. 1(c)].

A typical image resulting from the separation procedure, averaged over many repetitions, is plotted in Fig. 2(a). This set of data involves an average of 75 DTB pairs produced in each repetition. The averaged image shows the remaining BEC at the center and four DTB zones, L_-, R_-, L_+, R_+ (black boxes), defined by the two transverse states $|L\rangle$ and $|R\rangle$ and the two longitudinal momenta $\pm k_0$. We consider the correlations among two signals contained in any pair of the black boxes defined in Fig. 2(a). This defines a certain number of combinations of two DTB modes, each of which is labeled with an index [see Fig. 2(b)]. For each combination of modes, we compute the value of the number-squeezing parameter:

$$\xi^2 = \frac{\Delta S_-^2}{\Delta_b S_-^2} - \xi_n^2, \tag{2}$$

where ΔS_-^2 represents the variance of the signal difference S_- between the two boxes considered, $\Delta_b S_-^2$ denotes the corresponding binomial variance, and ξ_n^2 the noise contribution to the squeezing parameter (see the Supplemental Material [23]). A value of $\xi^2 < 1$ defines a number-squeezed emission.

In Fig. 2(c), the number-squeezing value ξ^2 is displayed as vertical bars as a function of the different combinations of DTB modes considered (the actual values are also expressed in Table I). We observe that the different combinations of DTB modes can be classified in three groups depending on the value of the number squeezing: (a) $\xi^2 \approx 0$ for $LL, RR, long$, (b) $\xi^2 \approx 1$ for $LR, RL, R\_L\_$, and (c) $\xi^2 \approx 2$ for *trans*. The group (a) refers to correlations between atoms that have opposite longitudinal momenta and belong to the same waveguide (LL or RR) or to any of them (*long*). This characteristic defines atoms belonging to the same twin pair [see Eq. (1)]; hence we find $\xi^2 < 1$. The group (b) refers to atoms that do *not* belong to the same twin pair, either because these combinations of DTB modes mix different waveguides (LR and RL) or because they consider atoms with the same longitudinal momenta ($R\_L\_$); hence the signals are uncorrelated and we find $\xi^2 \approx 1$. The last group (c) contains the combination *trans*, which compares the *total* signal between the L and R waveguides. Given the state in Eq. (1), we expect twin *pairs* to be detected either in the L or in the R waveguide, without correlation between these two modes. However, each atom is part of a twin pair, so the *atom* detection is not *trans*

TABLE I. Number squeezing. Noise-corrected atom number squeezing for different combinations of the four DTB modes.

t_{hold} (ms)	ξ^2_{LL}	ξ^2_{RR}	ξ^2_{LR}	ξ^2_{RL}	$\xi^2_{L\_R\_}$	ξ^2_{trans}	ξ^2_{long}	ξ^2_n
0.025	0.11	0.12	1.14	1.14	1.13	2.19	0.10	0.078
0.425	0.19	0.19	1.13	1.07	1.12	2.07	0.14	0.076

uncorrelated. In terms of the statistics of individual atoms, we find $\xi^2_{trans} = 2$ (see also the Supplemental Material [23]).

These results are compatible with the generation of a maximally entangled state as in Eq. (1), but also with a two-particle mixed state of $|L\rangle_-|L\rangle_+$ and $|R\rangle_-|R\rangle_+$. To exclude this case we need to look at the two-particle interference pattern.

Interference procedure.—In our experiment, each twin pair can be emitted in either the L or R waveguide. These represent two two-particle quantum paths that interfere with equal amplitude (balanced double well) when performing an interference measurement procedure; i.e., we avoid imprinting an extra transverse acceleration [Fig. 1(c)]. Unlike the single-particle case where an interference pattern is visible already in the mean density in momentum space (one-particle property), in the two-particle case we need to look at two-particle properties in order to extract information on the final state [17].

If the DTB emission preserves the coherence of the quasi-BEC, the DTB state shows two-atom interference in the second-order correlation function $g^{(2)}(k^y_-, k^y_+)$ linking atoms of opposite momenta:

$$g^{(2)}(k^y_-, k^y_+) = \frac{\langle n(k_y, -k_0) n(k_y, +k_0)\rangle}{\langle n(k_y, -k_0)\rangle \langle n(k_y, +k_0)\rangle}, \qquad (3)$$

where k_y is the transverse wave vector and $n(k_y, \pm k_0)$ is the single-particle density profile along the transverse axis at the two longitudinal momenta $\pm k_0$. The particular fringe pattern in $g^{(2)}(k^y_-, k^y_+)$ depends on the underlying density matrix associated to the DTB state [17]. Maximal contrast requires identifying the partners in each atom pair. In a low-pair emission regime, we emit an average of 10 DTB pairs in each experimental run. Averaging over the pairs will reduce the contrast in the observed interference.

In Figs. 3(a) and 3(b), we compare the simulated unnormalized $G^{(2)}(k^y_-, k^y_+) = \langle n(k_y, -k_0) n(k_y, +k_0)\rangle$ and experimental $g^{(2)}_{\text{expt}}(k^y_-, k^y_+)$ patterns: Fig. 3(a) shows the theoretical fringe pattern assuming a two-particle state of the form Eq. (1); Fig. 3(b) shows the experimental $g^{(2)}_{\text{expt}}(k^y_-, k^y_+)$ pattern averaged over 1498 experimental runs. The number of visible fringes depends on the value of the wells spacing $2y_0$ between the two potential waveguides. In order to compare the theoretical pattern (a) with the experimental one (b), we use $2y_0 = 1.3$ μm. This value is obtained from a simulation of the final double-well potential that was calibrated to match with the experiment.

The white box in Fig. 3(b) defines the integration area for the profiles in Fig. 3(c): the double arrow defines the integration axis, while the single arrow illustrates the transverse momentum coordinate k_y [horizontal axis in Fig. 3(c)]. The projected pattern shows clear fringes with a period consistent with the double well and a contrast $C = 0.032 \pm 0.004$. In order to ensure that the central fringe is not originating from the envelope, we compare the fringe profile with the mean profile obtained considering only the product of the independently averaged profiles $\langle n(k_y, -k_0)\rangle\langle n(k_y, +k_0)\rangle$ (blue dashed curve).

This fringe pattern in the measured $g^{(2)}(k^y_-, k^y_+)$ [Figs. 3(b) and 3(c)] combined with the absence of an interference fringe in the single-particle density is one of the central results of our experiment and it constitutes direct evidence for genuine two-particle interference. For a statistical mixture of the states $|L\rangle_-|L\rangle_+$ and $|R\rangle_-|R\rangle_+$, one would expect a flat profile $g^{(2)}(k^y_-, k^y_+) = 1$. Combined with the measurements of the number-squeezing correlations between the four guided DTB modes in Table I and following Ref. [17], our experiment shows that a significant

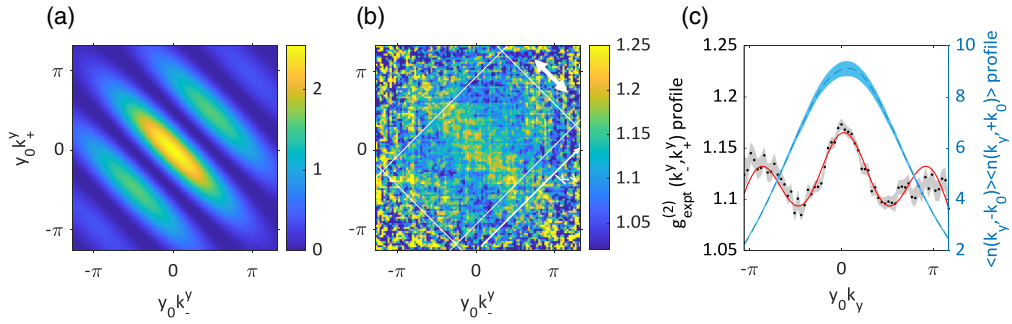

FIG. 3. Two-particle interference pattern. (a) Theoretical unnormalized $G^{(2)}(k^y_-, k^y_+) = \langle n(k_y, -k_0) n(k_y, +k_0)\rangle$ pattern assuming a DTB state of the form Eq. (1). (b) Experimental $g^{(2)}_{\text{expt}}(k^y_-, k^y_+)$ pattern. This set of data involves 1498 experimental runs, where each run contains 700–760 total atoms, 20 of which are DTB atoms (10 pairs), on average. (c) One-dimensional mean profiles obtained from averaging along the diagonal within the white box superimposed in Fig. 3(b). The mean antidiagonal profile of $g^{(2)}_{\text{expt}}(k^y_-, k^y_+)$ (black dots) is compared to the mean antidiagonal profile of $\langle n(k_y, -k_0)\rangle\langle n(k_y, +k_0)\rangle$ (light blue curve). The red curve represents a fit of the data from which we extract a value of the contrast of the two-atom interference $C = 0.032 \pm 0.004$. Units are scaled by the diagonal $\sqrt{2}$ factor and then normalized by the wells spacing $2y_0 = 1.3$ μm. The shaded areas represent the standard error of the mean.

fraction of atom pairs are emitted in the maximally entangled state of Eq. (1). This is a "lucky" situation where the reconstruction of the full density matrix of the two-particle state (and hence an entanglement demonstration) is in principle possible without any phase rotation, just by looking at the two-particle interference pattern [17]. We attribute the low contrast of $C = 0.032 \pm 0.004$ in our present experiment to the relatively large number of 10 pairs emitted on average in each measurement, thereby washing out the interference pattern.

Our experiments show a path toward a quantitative demonstration of entanglement for propagating atom beams in such a system as suggested in Ref. [17]. In order to achieve this goal we need to significantly increase the contrast of the two-particle interference, which will require a more detailed study of the emission process and better control over the number of emitted pairs, down to experiment with single pairs. A phase shift can be applied to the propagating DTBs by tilting the double-well potential to introduce an energy difference between the left- and right-well states, as in Ref. [34]. As an alternative procedure, one could implement Bragg deflectors as in Refs. [12,16] to rotate the state after its generation.

As a more general outlook, we see a huge potential in exploring nonlinear matter-wave optics for atoms propagating in waveguides and integrated matter-wave circuits. The processes behind the twin-atom emission are closely related to the matter-wave equivalents of parametric amplification and four-wave mixing. We envision the development of nonlinear matter-wave quantum optics. The creation of entangled atom-laser beams in twin-beam emission above threshold would be one directly accessible example.

We thank M. Pigneur and R. Trubko for help in the initial phases of the project, K. Nemoto and W. J. Munro for numerous inspiring discussions, and C. Lévêque for help with the manuscript. This work was funded by the Austrian Science Fund (FWF) via the QUANTERA project CEBBEC (I 3759-N27) and M. M. and P. H. acknowledge support by the project LATIN (Y-1121). I. M. acknowledges the support by the Wiener Wissenschafts- und Technologiefonds (WWTF) via Grant No. MA16-066 (SEQUEX) and by the Austrian Science Fund (FWF) via Grant No. SFB F65 (Complexity in PDE systems). T. Z. is supported by the EU's Horizon 2020 program under the M. Curie Grant No. 765267 (QuSCo). F. B., M. M., and T. Z. acknowledge the support from CoQuS. M. B. was supported by the EU through the M. Curie Grant ETAB (MSCA-IF-2014-EF 656530) and by the Austrian Science Fund (FWF) through the Lise Meitner Grant CoPaNeq (M2088-M27). S. M. acknowledges support from the Italian PRIN 2017. T. C. and S. M. acknowledge the support of the EC Quantum Flagship project PASQUANS.

[1] J. P. Dowling and G. J. Milburn, Quantum technology: the second quantum revolution, Phil. Trans. R. Soc. A **361**, 1655 (2003).
[2] European quantum flagship—Strategic research agenda, https://qt.eu//app/uploads/2020/04/Strategic_Research-_Agenda_d_FINAL.pdf.
[3] J.-W. Pan, Z.-B. Chen, C.-Y. Lu, H. Weinfurter, A. Zeilinger, and M. Żukowski, Multiphoton entanglement and interferometry, Rev. Mod. Phys. **84**, 777 (2012).
[4] M. Lamehi-Rachti and W. Mittig, Quantum mechanics and hidden variables: A test of Bell's inequality by the measurement of the spin correlation in low-energy proton-proton scattering, Phys. Rev. D **14**, 2543 (1976).
[5] B. Hensen, H. Bernien, A. E. Dréau, A. Reiserer, N. Kalb, M. S. Blok, J. Ruitenberg, R. F. Vermeulen, R. N. Schouten, C. Abellán *et al.*, Loophole-free Bell inequality violation using electron spins separated by 1.3 kilometres, Nature (London) **526**, 682 (2015).
[6] M. A. Rowe, D. Kielpinski, V. Meyer, C. A. Sackett, W. M. Itano, C. Monroe, and D. J. Wineland, Experimental violation of a Bell's inequality with efficient detection, Nature (London) **409**, 791 (2001).
[7] M. Ansmann, H. Wang, R. C. Bialczak, M. Hofheinz, E. Lucero, M. Neeley, A. O'Connell, D. Sank, M. Weides, J. Wenner *et al.*, Violation of Bell's inequality in Josephson phase qubits, Nature (London) **461**, 504 (2009).
[8] W. Rosenfeld, D. Burchardt, R. Garthoff, K. Redeker, N. Ortegel, M. Rau, and H. Weinfurter, Event-Ready Bell Test Using Entangled Atoms Simultaneously Closing Detection and Locality Loopholes, Phys. Rev. Lett. **119**, 010402 (2017).
[9] R. Bücker, J. Grond, S. Manz, T. Berrada, T. Betz, C. Koller, U. Hohenester, T. Schumm, A. Perrin, and J. Schmiedmayer, Twin-atom beams, Nat. Phys. **7**, 608 (2011).
[10] M. Bonneau, J. Ruaudel, R. Lopes, J.-C. Jaskula, A. Aspect, D. Boiron, and C. I. Westbrook, Tunable source of correlated atom beams, Phys. Rev. A **87**, 061603(R) (2013).
[11] R. Lopes, A. Imanaliev, A. Aspect, M. Cheneau, D. Boiron, and C. I. Westbrook, Atomic Hong–Ou–Mandel experiment, Nature (London) **520**, 66 (2015).
[12] P. Dussarrat, M. Perrier, A. Imanaliev, R. Lopes, A. Aspect, M. Cheneau, D. Boiron, and C. I. Westbrook, Two-Particle Four-Mode Interferometer for Atoms, Phys. Rev. Lett. **119**, 173202 (2017).
[13] J.-C. Jaskula, M. Bonneau, G. B. Partridge, V. Krachmalnicoff, P. Deuar, K. V. Kheruntsyan, A. Aspect, D. Boiron, and C. I. Westbrook, Sub-Poissonian Number Differences in Four-Wave Mixing of Matter Waves, Phys. Rev. Lett. **105**, 190402 (2010).
[14] D. K. Shin, B. M. Henson, S. S. Hodgman, T. Wasak, J. Chwedeńczuk, and A. G. Truscott, Bell correlations between spatially separated pairs of atoms, Nat. Commun. **10**, 4447 (2019).
[15] J. Kofler, M. Singh, M. Ebner, M. Keller, M. Kotyrba, and A. Zeilinger, Einstein-Podolsky-Rosen correlations from colliding Bose-Einstein condensates, Phys. Rev. A **86**, 032115 (2012).
[16] R. J. Lewis-Swan and K. V. Kheruntsyan, Proposal for a motional-state Bell inequality test with ultracold atoms, Phys. Rev. A **91**, 052114 (2015).

[17] M. Bonneau, W. J. Munro, K. Nemoto, and J. Schmiedmayer, Characterizing twin-particle entanglement in double-well potentials, Phys. Rev. A **98**, 033608 (2018).
[18] D. S. Petrov, G. V. Shlyapnikov, and J. T. M. Walraven, Regimes of Quantum Degeneracy in Trapped 1D Gases, Phys. Rev. Lett. **85**, 3745 (2000).
[19] R. Folman, P. Krüger, D. Cassettari, B. Hessmo, T. Maier, and J. Schmiedmayer, Controlling Cold Atoms using Nanofabricated Surfaces: Atom Chips, Phys. Rev. Lett. **84**, 4749 (2000).
[20] T. Schumm, S. Hofferberth, L. M. Andersson, S. Wildermuth, S. Groth, I. Bar-Joseph, J. Schmiedmayer, and P. Krüger, Matter-wave interferometry in a double well on an atom chip, Nat. Phys. **1**, 57 (2005).
[21] S. Hofferberth, I. Lesanovsky, B. Fischer, J. Verdu, and J. Schmiedmayer, Radiofrequency-dressed-state potentials for neutral atoms, Nat. Phys. **2**, 710 (2006).
[22] I. Lesanovsky, T. Schumm, S. Hofferberth, L. M. Andersson, P. Krüger, and J. Schmiedmayer, Adiabatic radio-frequency potentials for the coherent manipulation of matter waves, Phys. Rev. A **73**, 033619 (2006).
[23] See Supplemental Material at http://link.aps.org/supplemental/10.1103/PhysRevLett.126.083603 for more details on state inversion using optimal-control techniques, theoretical calculation of the expected two-particle state, possible extension to a fermionic system, the imaging setup, and detection noise, which includes Refs. [24–30].
[24] A. Basden, C. Haniff, and C. Mackay, Photon counting strategies with low-light-level CCDs, Mon. Not. R. Astron. Soc. **345**, 985 (2003).
[25] S. van Frank, A. Negretti, T. Berrada, R. Bücker, S. Montangero, J.-F. Schaff, T. Schumm, T. Calarco, and J. Schmiedmayer, Interferometry with non-classical motional states of a Bose–Einstein condensate, Nat. Commun. **5**, 4009 (2014).
[26] S. van Frank, M. Bonneau, J. Schmiedmayer, S. Hild, C. Gross, M. Cheneau, I. Bloch, T. Pichler, A. Negretti, T. Calarco *et al.*, Optimal control of complex atomic quantum systems, Sci. Rep. **6**, 34187 (2016).
[27] T. Caneva, T. Calarco, and S. Montangero, Chopped random-basis quantum optimization, Phys. Rev. A **84**, 022326 (2011).
[28] R. Bücker, Twin-atom beam generation in a one-dimensional Bose gas, Ph.D. thesis, Techische Universität Wien, 2013.
[29] M. Pigneur, *Non-Equilibrium Dynamics of Tunnel-Coupled Superfluids: Relaxation to a Phase-Locked Equilibrium State in a One-Dimensional Bosonic Josephson Junction* (Springer, Vienna, 2020).
[30] B. Zhao, Z.-B. Chen, J.-W. Pan, J. Schmiedmayer, A. Recati, G. E. Astrakharchik, and T. Calarco, High-fidelity entanglement via molecular dissociation in integrated atom optics, Phys. Rev. A **75**, 042312 (2007).
[31] F. Gerbier, Quasi-1D Bose-Einstein condensates in the dimensional crossover regime, Europhys. Lett. **66**, 771 (2004).
[32] R. J. Lewis-Swan and K. V. Kheruntsyan, Atomic twin beams and violation of a motional-state Bell inequality from a phase-fluctuating quasicondensate source, Phys. Rev. A **101**, 043615 (2020).
[33] R. Bücker, A. Perrin, S. Manz, T. Betz, C. Koller, T. Plisson, J. Rottmann, T. Schumm, and J. Schmiedmayer, Single-particle-sensitive imaging of freely propagating ultracold atoms, New J. Phys. **11**, 103039 (2009).
[34] M. Pigneur, T. Berrada, M. Bonneau, T. Schumm, E. Demler, and J. Schmiedmayer, Relaxation to a Phase-Locked Equilibrium State in a One-Dimensional Bosonic Josephson Junction, Phys. Rev. Lett. **120**, 173601 (2018).

Correction: The article identification number in Ref. [14] contained an error and has been fixed, enabling access to the online article.